water

MDPI

Article

Potential of Sentinel Images to Evaluate Physicochemical Parameters Concentrations in Water Bodies—Application in a Wetlands System in Northern Colombia

César Padilla-Mendoza [1], Franklin Torres-Bejarano [1,*], Gabriel Campo-Daza [1] and Luis Carlos González-Márquez [2]

[1] Environmental Engineering Department, Universidad de Córdoba, Montería 230002, Colombia
[2] Engineering and Technology Department, Universidad Autónoma de Occidente, Unidad Regional Guasave, Guasave 81048, Sinaloa, Mexico
* Correspondence: franklintorres@correo.unicordoba.edu.co

Abstract: This research demonstrated the feasibility of applying Sentinel-2 images to generate empirical models and estimate physicochemical parameters concentration, particularly nutrients in the wetland system called Bajo Sinú wetlands complex, Colombia. Spearman correlations were determined between water quality parameters, which were monitored at 17 points in the wetland on 5 February 2021, with Sentinel-2 images reflectance values from the same monitoring date; the correlations allowed the identification of statistically significant bands in the multiple linear regression algorithm implementation to determine empirical water quality models. The results show significant correlations between the optically active parameters, TSS-Turbidity, which in turn correlated with the optically inactive parameters Turbidity-NO_3 and TSS-DO, as well as non-optically active parameters among themselves, TDS-NO_3 and TDS-TP; the empirical models presented higher than 74.5% fit (R^2), particularly DO (R^2 = 0.948), NO_3 (R^2 = 0.858) and TP (R^2 = 0.779) were the models with the highest fits (R^2). These models allowed us to properly estimate the spatial distribution of nutrient-forming compounds in the wetlands complex. The determinant role played by turbidity in this type of water body is highlighted; it acts as a connecting constituent that makes the estimation of water quality parameters without spectral response through remote sensing feasible. Sentinel-2 images and multiple linear regression algorithms have been shown to be effective in estimating the concentration of water quality parameters without spectral response, such as NO_3 and TP in shallow tropical wetlands, due to the processes of transformation, interaction and dependence between the different environmental variables in aquatic ecosystems.

Keywords: wetlands; water quality models; remote sensing

Citation: Padilla-Mendoza, C.; Torres-Bejarano, F.; Campo-Daza, G.; González-Márquez, L.C. Potential of Sentinel Images to Evaluate Physicochemical Parameters Concentrations in Water Bodies—Application in a Wetlands System in Northern Colombia. *Water* **2023**, *15*, 789. https://doi.org/10.3390/w15040789

Academic Editor: Guangxin Zhang

Received: 20 October 2022
Revised: 30 January 2023
Accepted: 1 February 2023
Published: 17 February 2023

1. Introduction

Wetlands are land extensions with saturated or water-covered soils characterized by almost zero velocities. These systems are of great ecological importance because they host an important diversity of species and provide cultural, water-regulating, and agricultural and fisheries provisioning ecosystem services, which, if well managed, boost the nearby population's economy [1,2]. They also play an important role in nutrient and sediment retention, due to the different biogeochemical processes involved and the retention periods that change depending on their hydrological variability [3–6].

For these reasons, nutrient analysis becomes more relevant in these ecosystems [7]. In recent decades, intense human activities resulting from the urban centers' increase in number and size and agro-industrial development have caused many surface and groundwater systems to be polluted by wastewater (treated and untreated), agricultural runoff and the increased use of nutrient-rich fertilizers [8]. This has caused and accelerated

water bodies' eutrophication, becoming the most serious and widespread problem in aquatic ecosystems worldwide [6,9–12].

Other consequences of increased nutrients in wetlands include hindering the optimal growth of fish species [13] and fostering conditions for a rise in the population density of floating macrophytes [14], as observed in the Bajo Sinú Complex during monitoring.

For nutrients in tropical wetlands study, constant monitoring has been carried out to characterize the biochemical cycle of nitrogen and phosphorus in water due to the high complexity of interrelationships with the surrounding biomass [15]; some authors analyze the mechanisms of nitrogen and phosphorus retention and accumulation in wetlands [16,17], these studies with conventional nutrient monitoring have the limitations of small scales and high economic investment [18].

In situ water quality sampling is limited to a local scale, and conventional analytical methods used to analyze nitrogen and phosphorus compounds, although widely used, are expensive and require a lot of manpower [19]. In addition, due to the limited mobility in wetlands because of their shallow depth and presence of aquatic plants, accessing the entire water surface is difficult, hindering sampling and data collection and increasing the cost and time invested in water quality monitoring [20–22]. Therefore, remote sensing can increase the availability of data for proper water quality assessment by providing two-dimensional maps derived from geographic information systems that would otherwise require a large number of in situ water quality monitoring stations [8]. Likewise, different studies have shown the usefulness of remote sensing for estimating nutrient concentrations in water bodies [8,23,24].

For several decades, remote sensing has been applied to assess the state of water quality in inland and coastal surface ecosystems using different remote sensors, with Landsat being the most widely applied sensor, both for optically active (e.g., suspended solids, chlorophyll, turbidity) and inactive (e.g., nutrients, dissolved oxygen) parameters [24–28]. MODIS images have also been of great application for the study of different water quality parameters in coastal and inland areas [29,30]. Recently, the use of Sentinel 2 images has shown potential for water quality analysis. Several authors have used Sentinel 2 images to correlate Secchi disk depth and chlorophyll a [31,32], evaluate field parameters [33] describe coastal lagoon dynamics [34], and map coral reefs [35].

Although nutrients (nitrates and phosphates) have no spectral response they can be systematically linked in aquatic environments according to their main characteristics concerning other water quality parameters [8]. Their concentration can be correlated with optically active parameters such as chlorophyll [36,37], transparency [20,38,39], turbidity, and total suspended solids [40].

Water quality parameters analysis in wetlands using satellite images helps to understand their spatial and temporal variability, sometimes identifying nutrients' behavior in water; from another perspective, it is an economical technique that allows constant and rapid monitoring to support decision-making [33,41]; furthermore, it serves as a complement to monitoring programs [34].

In Colombia, objectives for a good ecological state of rivers, lakes and coastal waters have not been proposed as in European countries [42]. However, the National Policy for Inland Wetlands of Colombia (PNHIC in Spanish) has as one of its goals the preservation of wetlands important for biodiversity conservation at the regional and national level; and eutrophication is one of the main disturbance factors to mitigate; therefore, there is a specific goal to carry out water quality monitoring that includes nutrients [43,44].

In light of this, in this research, the objective was to show the feasibility of applying Sentinel-2 images to generate empirical models and estimate nutrient concentration in northern Colombian wetlands. The models were generated from the relationship between nitrate (NO_3), total phosphorous (TP), total Suspended Solids (TSS), turbidity, total dissolved solids (TDS), and dissolved oxygen (DO) concentrations measured in the wetland and the reflectance recorded in Sentinel-2A images obtained for the Bajo Sinú wetlands complex, Colombia.

2. Materials and Methods

2.1. Study Area

The Bajo Sinú Wetlands Complex is made up of a group of wetlands located in the north of the department of Córdoba, Colombia. This complex was declared a protected area in the category of Regional District of Integral Management of Natural Resources by the Regional Autonomous Corporation of the Sinú and San Jorge Valleys (CVS for its acronym in Spanish) through agreement No. 76 of 25 October 2007, due to its ecological and economic importance [45].

The research was carried out specifically in the Guartinaja (G), Sapal (S) and Momil (M) wetlands (Figure 1), which at the time of sampling (5 February 2021) had areas of 27.10 km^2, 2.96 km^2 and 6.63 km^2 respectively. These water bodies are delimited by the municipalities of Lorica, with a population of 115,461, Purísima with 17,587 inhabitants, Momil with 20,117 inhabitants, and Chimá, with a population of 17,905, according to data from the National Administrative Department of Statistics (DANE for its acronym in Spanish) [46].

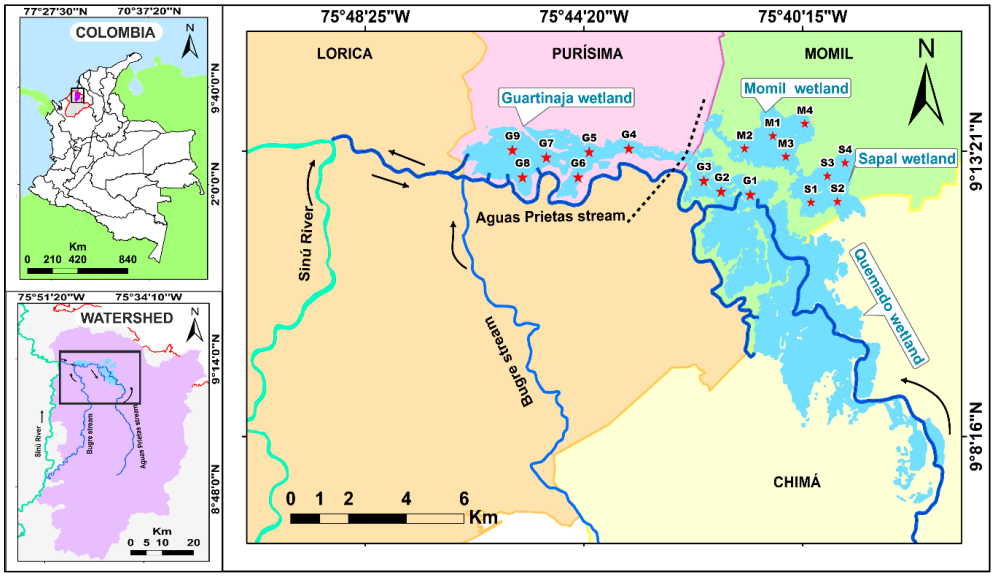

Figure 1. Wetland's complex location and sampling sites.

The wetlands complex receives inputs from the Bugre and Aguas Prietas streams, which are characterized by their low water velocities when approaching the floodplain, showing a quasi-lotic behavior in dry periods [47].

The Aguas Prietas stream has a bidirectional behavior in the section from the Guartinaja wetland to the Sinú River, which means that during periods of high water levels, it delivers water to the Sinú River with flows of up to 245 m^3/s; and during the summer, it receives water from the river with flows of up to 80 m^3/s [48]. In its upstream section, near Chimá municipality, the Aguas Prietas stream carries an average flow of approximately 10 m^3/s. The Bugre stream flow rates are lower, transporting an average of approximately 50 m^3/s [48].

The wetlands complex basin has minimum multiannual precipitation of 1206.44 mm, a maximum of 1579 mm, and an annual average of 1395.5 mm, with a wet period from early April to late October; the average temperature within the basin is 27.5 °C, the average annual evapotranspiration 1300 mm, and surface wind speed 2.5 m/s (http://dhime.ideam.gov.co/, accessed on 19 September 2022).

2.2. Environmental Data Analysis

For water quality monitoring, 17 measurement and sampling stations were distributed in the wetlands: 9 in Guartinaja, 4 in Sapal, and 4 in Momil (Figure 1). The measurement and sampling campaign was conducted on 5 February 2021 to coincide with the moment

the Sentinel-2 satellite would capture the image. In situ measurements of dissolved oxygen (DO), turbidity, and total dissolved solids (TDS) were taken at all stations using a calibrated Hanna model HI9829 multiparameter [49]. In the laboratory, total suspended solids (TSS) were analyzed by the SM 2540 D method, total phosphorus (TP) by SM 4500-P B.4 and SM 4500-P E methods, and nitrate (NO_3) by the SM 4500-NO_3-B method.

Turbidity and TDS were chosen because these parameters allow determining the amount of both dissolved and suspended solids in the water column, and, consequently, because they have active optical properties, they can be correlated with other optically non-active parameters, such as those described below. By measuring DO, the effective amount of gaseous oxygen in water bodies, which is vital for aquatic organisms, is known. With TP, the forms of reactive phosphorus, dissolved, and organic particle fractions are quantified. Moreover NO_3 was chosen considering that around the studied wetland system, there are agricultural and livestock areas that generate direct, diffuse inputs of dissolved nitrate to the water body due to runoff.

For the water samples collection and transport, the guide for monitoring discharges, surface water, and groundwater weas used [50]. Samples were collected in 1 L glass bottles at approximately 0.3 m depth from the water surface, then stored and refrigerated at 4 °C in a portable cooler for transport to the laboratory.

2.3. Satellite Data Source

Satellite data from the Sentinel-2 mission multispectral instrument (MSI), consisting of the Visible and Near-Infrared (VNIR) and Short-Wave Infrared (SWIR) bands, were used (Table 1). The Sentinel-2A image was downloaded from the Copernicus Open Access Hub platform with radiometric and atmospheric corrections [51]. All bands used in this study with a 20 m spatial resolution were standardized to 10 m.

Table 1. Sentinel-2 bands description.

Band	Function	Wavelength (nm)	Bandwidth (nm)	Resolution (m)
1	Coastal aerosol	443	20	60
2	Blue	490	65	10
3	Green	560	35	10
4	Red	665	30	10
5	infrared- NIR 1	705	15	20
6	NIR 2	740	15	20
7	NIR 3	783	20	20
8	NIR 4	842	115	10
8A	infrared narrow (NIRn)	865	20	20
9	Water vapor	945	20	60
10	Cirrus	1380	30	60
11	SWIR 1	1610	90	20
12	SWIR 2	2190	180	20

2.4. Statistical Analysis

The Shapiro-Wilk test was performed, and its results showed that several parameters did not present normality; therefore, a Spearman's bilateral correlation test (r) was performed, applicable when the data are not normal, where an (r) equal or close to (1) represents parameters with direct correlation. Alternatively, values equal or close to (-1) represent indirect relationships, being a null correlation that whose value of (r) is equal to zero. These analyses were performed with R software version 4.1.2.

Water quality parameter estimation models were generated and validated by implementing a multiple linear regression technique in Matlab R2021a software [52,53]. To construct the multiple regression models, bands and band ratios that indicated a good correlation with water quality parameters were selected.

The models were selected taking into account the best correlation values, the determination coefficient (R^2), and the root mean square error (RMSE) between the observed and estimated values. These parameters indicate the model's importance and the relationship nature between the variables [41]. In addition, regression graphs were created to verify the relationship between the data observed as independent variables and those estimated by the model as the dependent variable.

2.5. Water Quality Parameters Maps

Initially, wetlands contours were extracted from the Sentinel-2A image by applying the Normalized Difference Water Index (NDWI). Then, with the QGIS software version 3.16 raster calculator, the generated statistical models were applied to obtain the spatial distribution maps of the water quality parameters' estimated concentration.

3. Results

3.1. Water Quality Parameters

Table 2 summarizes the main statistics values obtained for the different water quality parameters measured in the stations of Guartinaja (G), Sapal (S), and Momil (M) in the wetlands complex.

Table 2. Main statistics (mean, range, and standard deviation) for the following water quality parameters: nitrate (NO_3), total phosphorus (TP), total suspended solids (TSS), turbidity, total dissolved solids (TDS), and dissolved oxygen (DO) measured during the field study.

Main Statistics	Turbidity NTU	TDS mg/L	DO mg/L	TSS mg/L	TP mg/L	NO_3 mg/L
Maximum	33.8	225.9	7.9	34.0	0.170	2.35
Minimum	6.5	175.9	5.1	4.5	0.050	0.86
Mean	18.8	202.1	5.9	18.1	0.117	1.62
Median	20.6	206.9	5.7	16.3	0.120	1.63
SD	10.3	19.1	0.8	10.9	0.040	0.56

DO mean and standard deviation (mean ± SD) was 5.9 ± 0.8 mg/L with a minimum value of 5.1 mg/L (station G5) and a maximum of 7.9 mg/L (station G9). The measured turbidity values were low, in the 6.5 (in M5) and 33.8 NTU range (in S5), with a mean of 18.8 ± 10.3 NTU. These DO and turbidity concentrations are similar to those reported by [33] for the same wetlands complex. TSS mean concentration in this study was 18.1 ± 10.9 mg/L with minimum values of 4.5 mg/L (in G5) and maximum values of 34 mg/L (in S5); The TDS mean obtained in this study was 197.2 ± 19.2 mg/L with maximum and minimum values of 175.9 and 225.9 mg/L. The TP showed a mean of 0.12 ± 0.04 mg/L with concentrations from 0.05–0.17 mg/L. NO_3 showed a concentration range between 0.86 (station S5) and 2.35 (at station G5) with a 1.62 ± 0.56 mg/L mean.

3.2. Correlation Analysis of Water Quality Parameters

Significant correlations were present between non-optically active parameters (Figure 2) TDS–NO_3 (r = 0.63) and TP–TDS (r = −0.65); this correlation was also shown by [40]. Other correlations between optically active and non-optically active parameters were observed; Turbidity–NO_3 (r = −0.71) showed a strong correlation, and similar results were obtained [54]. TSS–Turbidity showed a strong positive correlation (r = 0.71), also reported by [55]. Similar results were obtained by [56], who found that turbidity and TSS had strong positive correlations with each other. TSS–TP (r = −0.08) and TSS–NO_3 (r = −0.64) showed no significant correlation, a condition associated with the lack of constant water inflow due to the dry period [57].

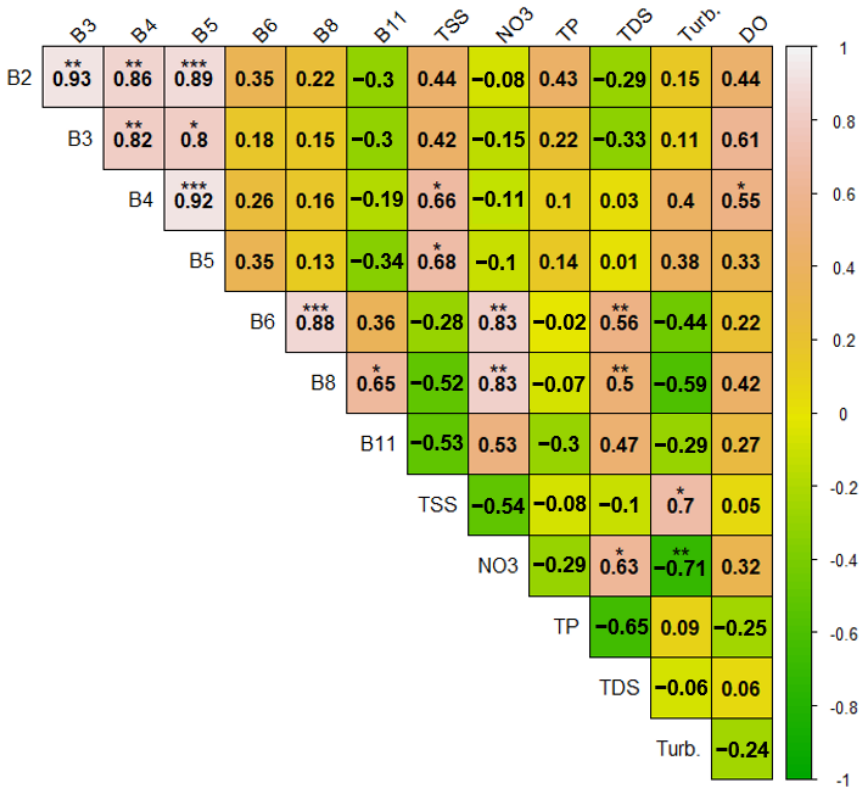

Figure 2. Spearman correlation correlogram; significance values at *** $p < 0.001$, ** $p < 0.01$, * $p < 0.05$.

3.3. Regression Models

Table 3 shows two models for each parameter, and the first is the best fit. It is observed that the optically active water quality parameter, TSS, was related to the visible (VIS) and near-infrared (NIR) electromagnetic spectrum bands, while turbidity was only related to the NIR bands. Similarly, parameters that have no spectral response, such as DO, TP, and TDS, were related to the VIS and NIR spectrum bands; however, NO_3 was only related to the NIR spectrum bands.

Table 3. Water quality models obtained from satellite image analysis.

WQP	Model Derived from Regression Analysis	R^2	RMSE
DO	**−39.2556 + 0.8061/B4 + 4288.3263 × (B4 × B5) + 19.4829 × (B4/B5)**	0.948	0.182
	−3.7611 + 57.4864 × B4 + 109.5176 × B8 + 4.0720 × (B4/B5)	0.754	0.394
Turbidity	**2787.4155 − 67370 × B6 + 76850 × B8 − 3160.9521 × (B8/B6)**	0.769	4.693
	191.1427 − 11.3280 × (1/B5) + 6150.3974 × (B4) − 96330 × (B4 × B5)	0.629	2.459
TDS	**191.4556 + 3475.4249 × B6 − 1449.3128 × B8 − 58.0480 × (B2/B8)**	0.783	4.482
	175.0792 + 2384.3749 × B6 − 50.7716 × (B2/B8)	0.773	8.66
TSS	**−52.5628 + 536.2086 × B5 + 30.2611 × (B4/B8)**	0.745	5.218
	30.2457 + 649.2762 × B4 − 80.0834 × (B8/B5) + 11.2173 × (B8/B4)	0.738	5.281
TP	**1.6130 − 0.030 × (1/B2) − 12.1973 × B6 − 0.2562 × (B4/B8)**	0.779	0.018
	1.4349 − 0.0276 × (1/B2) − 11.2153 × B8 − 0.2337 × (B4/B8)	0.688	0.021
NO_3	**−88.3612 + 2119.4812 × B6 − 2338.2696 × B8 + 99.7217 × (B8/B6)**	0.858	0.200
	1.8516 + 50.4735 × B6 + 9.1044 × B8 − 1.8144 × (B2/B8)	0.833	0.217

In addition, TSS, turbidity, and TDS had the NIR spectrum B8 band in common in their models similar to those results obtained by [58] and [33].

Considering the parameter pairs with the highest negative correlations, such as TDS-TP and Turbidity-NO_3, in their individual statistical models, the B2 band is inversely related to TP and directly related to TDS; however, the most influential bands, such as B8 and B6, showed a direct relationship in both parameters for each empirical model. A similar case occurs with the Turbidity and NO_3 parameters, which particularly, in their models, presented terms with the same bands (B8 and B6) and band ratio (B8/B6), but with different signs and coefficients; this evidences the relationship between optically active and non-active water quality parameters, considering the spectral bands found individually in each empirical model.

Overall, the obtained and selected multiple regression models showed an $R^2 > 0.7$ between the reflectance of Sentinel-2A spectral bands and the observed water quality values (Figure 3). The statistical models with the best determination coefficients were DO, TDS, and NO_3 with $R^2 > 0.78$ (Figure 3a,c,f). Turbidity, TSS, and TP models (Figure 3a,c) showed R^2 greater than 0.745.

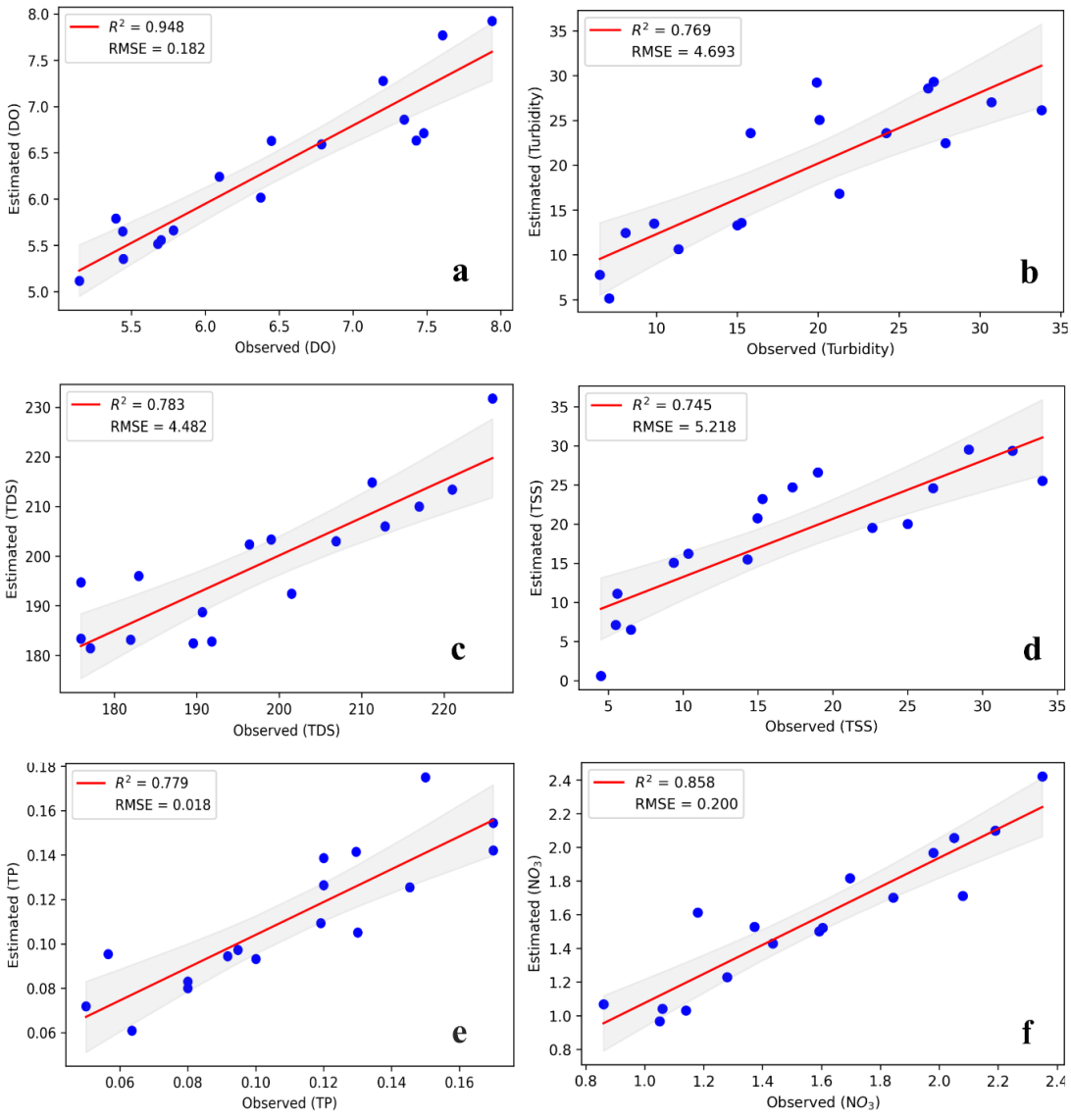

Figure 3. Correlation of observed vs. estimated data with the models. (**a**) dissolved oxygen (DO); (**b**) turbidity; (**c**) total dissolved solids (TDS); (**d**) total suspended solids (TSS); (**e**) total Phosphorus (TP) and (**f**) nitrates (NO_3).

3.4. Concentration Distribution Maps

By applying the empirical models to the Sentinel-2A image, DO, turbidity, TDS, TSS, TP, and NO_3 concentration maps of the Bajo Sinú wetlands complex were obtained (Figure 4). They help visualize the spatial concentration variation in the entire water body and produce relevant information for water resource management and water quality assessments.

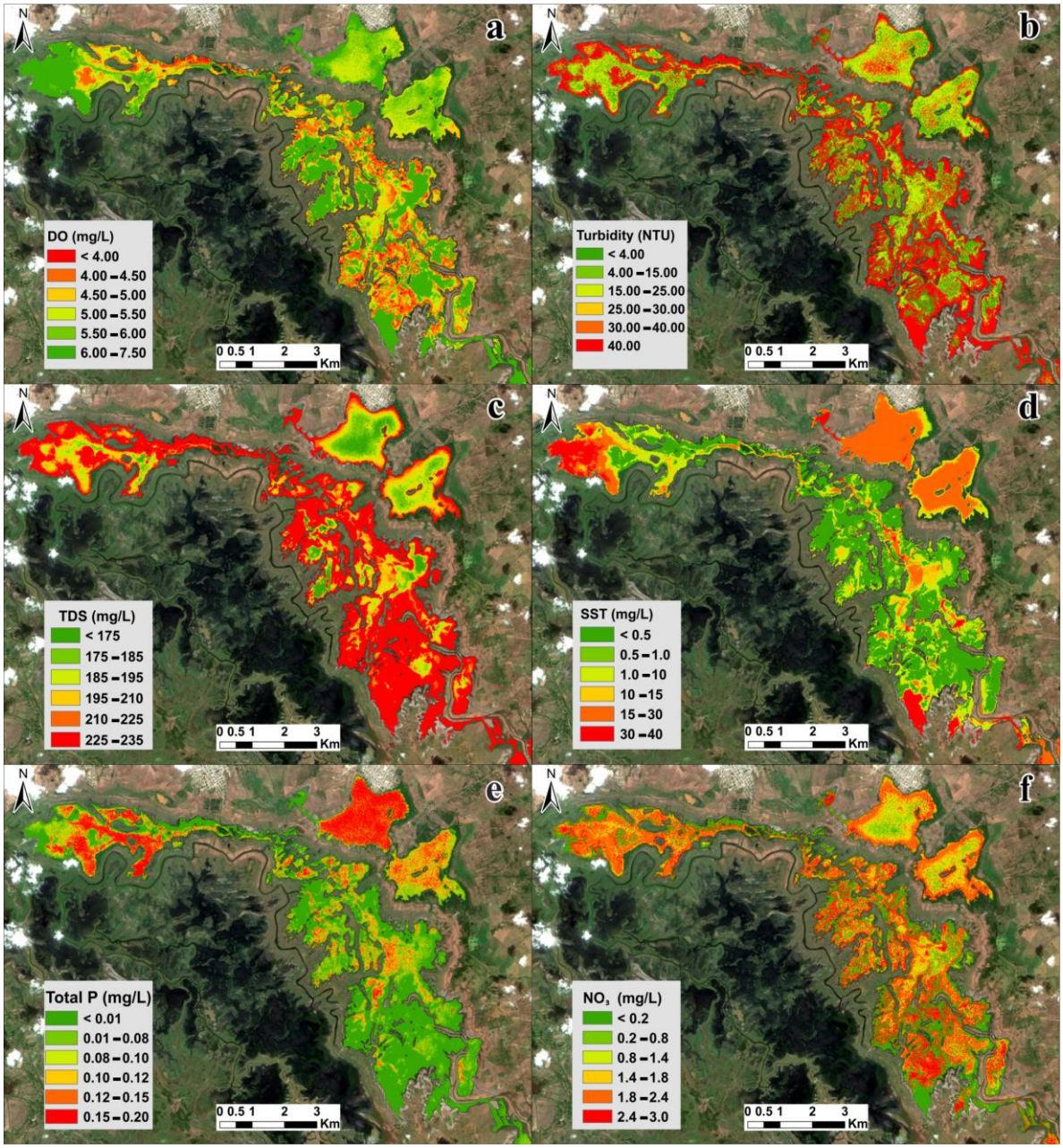

Figure 4. Water quality maps estimated from the models. (**a**) dissolved oxygen (DO); (**b**) turbidity; (**c**) total dissolved solids (TDS); (**d**) total suspended solids (TSS); (**e**) total Phosphorus (TP) and (**f**) nitrates (NO_3).

According to the DO concentration map (Figure 4a), it can be observed that the Guartinaja wetland has concentrations lower than 4 mg/L in the water body narrow zone. The Momil and Sapal wetlands have concentrations above 4.5 mg/L in a large part of their extension. However, in the Guartinaja wetland central area, between stations G7 and G8, estimated concentrations were below the quality criteria for flora and fauna preserva-

tion established in Decree 703 of 2018 of the Environment and Sustainable Development Sector, Colombia.

The study area in the measurement date was characterized by precipitation absence and wetlands' low water levels (<1.3 m); these conditions can increase retention times and influence nutrient concentrations variation in water bodies [7,59,60]. In the Guartinaja wetland, an abundant presence of *Najas arguta*, a very common plant in this wetland complex, was observed [61]; characteristics that also contribute to turbidity concentration decrease [56].

The TSS concentration map shows that high values in the Guartinaja wetland are observed to the northwest (Figure 4d); this location is close to the mouth of the Aguas prietas stream to the Sinú River. This behavior occurred because, at the time of sampling, the river was generating water inputs through the Aguas Prietas stream to the wetland, which caused the TSS increase. In the Momil and Sapal wetlands, TSS values are more homogeneous and are above 15 mg/L. The high sediment concentrations' most obvious effect on water quality is turbidity. TSS can increase during the rainy season and decrease in the absence of rain, becoming an important parameter to determine land use in a basin [55,62].

The Guartinaja wetland TDS concentrations (Figure 4c) show values ranging 195–210 mg/L in some areas and most of the water surface with values above 225 mg/L. This is explained by the shallow water depths and the wetland bottom nature [63]; on the contrary, the Momil and Sapal wetlands show concentrations ranging from 175 to 195 mg/L.

TP and NO_3 (Figure 4e,f) in the central Guartinaja wetland areas show homogeneous distributions with high concentrations. The predominant concentrations for TP (Figure 4e) are between 0.01 and 0.08 mg/L in the Guartinaja wetland; the northwestern sector values were above 0.15 mg/L; in the Momil wetland, concentrations were above 0.15 mg/L with a homogeneous distribution. However, for the Sapal wetland, the values were between 0.10 mg/L and 0.15 mg/L. NO_3 values on the Momil and Sapal wetlands shores are between 1.8 mg/L and 2.4 mg/L; however, in the central areas, they are between 0.8 mg/L and 1.4 mg/L (Figure 4f). In the Guartinaja wetland, NO_3 values were high, ranging between 1.8 mg/L and 3 mg/L, which could induce eutrophication processes in the wetlands. These nutrient values, compared to other studies in tropical wetlands, range from 0.0005 to 6 mg/L [64–70].

Some authors state that tributaries that feed this type of wetlands carry a load of nutrients from agricultural, domestic, industrial, and livestock activities [71–74]; several of these activities take place in the Bajo Sinú wetland complex basin and in the main municipalities that comprise it.

4. Discussions

4.1. Statistical Correlations between Physicochemical Parameters and Sentinel 2 Bands

Bands B4 and B5 presented a good correlation with TSS, which through B4, is related to DO. B6 and B8 bands showed a strong correlation with NO_3 and a moderate correlation with TDS (Figure 5). All the defined correlations presented a significance level of $p \leq 0.05$.

TSS has little influence on nitrogen; however, at high concentrations, they can influence PO_4 ion retention [75,76]. The relationships between TP with other parameters may vary according to the water body. Therefore, in this study, the linear correlation between TP and turbidity was not present; however, this does not mean that the correlation does not occur, as it may exist in a non-linear way, considering that the correlations are influenced by TP concentration, the depth of the water body, pH, and chlorophyll [77]. Turbidity can occur in both algal and inorganic forms, but in this wetland complex, turbidity is caused predominantly by inorganic substances and sediment inputs from the Sinú River through the Aguas Prietas stream [78]. Only Turbidity–NO_3 showed a direct correlation between an optical and a non-optically active parameter ($r = -0.71$).

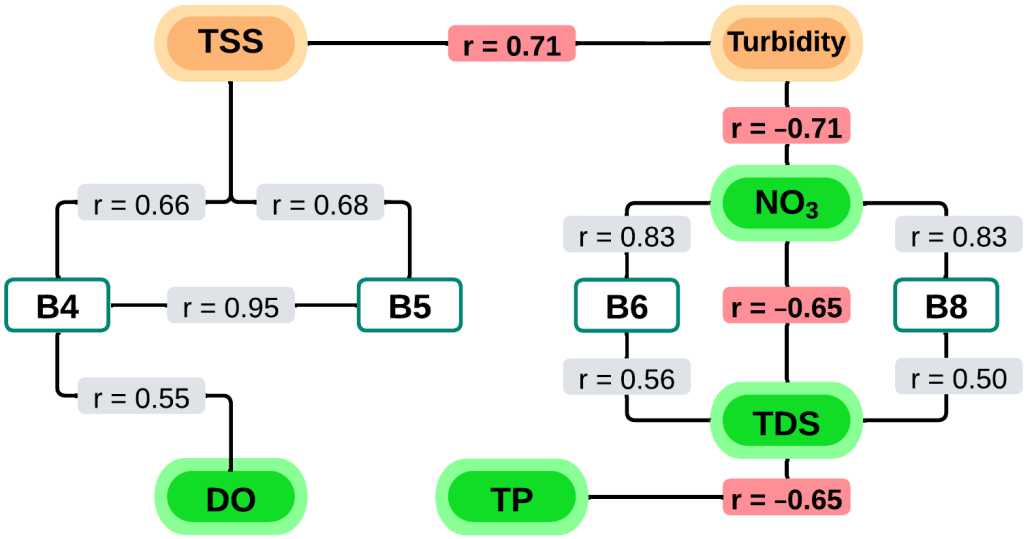

Figure 5. Relationship between analyzed water quality parameters and Sentinel-2A image bands.

For the TDS-NO_3 correlation, bands B6 and B8 were directly related to each parameter in the empirical models. Therefore, with the correlations and empirical models, it is inferred that TSS and Turbidity concentrations, as optically active parameters [79,80], present indirect relationships through the Sentinel 2 image bands, with parameters difficult to extract spectral characteristics such as DO, NO_3, TDS, and TP [81,82].

For DO, a high relationship was obtained with the VIS and NIR spectrum B4 and B5 bands, with R^2 = 0.948 and RMSE = 0.182 mg/L (Table 2). The authors of [83] show that there is a relationship between the NIR-VIS spectrum bands and the DO, implementing other robust algorithms in the absence of spectral response [84].

The model obtained for TP was related to B2, B4, B6, and B8 bands. The authors [85] relate it in their TP model to the B2 band, which showed a linear combination with this parameter, and argue that, although it is an optically inactive molecule, its solubility in water and interaction with dissolved particles in the medium allows it to be related to other parameters that are optically active. Meanwhile, [86] showed that the VIS and NIR spectrum wavelengths correlate with this parameter using the multiple linear regression method.

The NO_3 model bands combination shows a strong relationship with B6 and B8 bands, i.e., with the NIR electromagnetic spectrum. Recently, [85] studied, through Landsat 8 images, the total nitrogen presence in water, obtaining a statistical model relating VIS and NIR wavelengths using deep learning techniques.

As for turbidity, the bands' linear combination with the best correlation was those relating B6 and B8 bands. The electromagnetic spectrum considered in the turbidity model followed the study conducted by [27], with the difference that in this new model, only the NIR spectrum bands were included.

Finally, TDS were associated with B2, B6, and B8 bands; the interrelationship with these bands may be associated with algae presence, suspended particles, and shallow water. These characteristics were present on the wetland complex's monitoring date, a condition that allows the water composition to be related to the VIS and NIR bands [87,88].

4.2. Water Quality Analysis

The values of DO mean that at all measurement points, the concentrations were above 2 mg/L, which is the minimum condition for sustaining aquatic life [89,90] and above hypoxia conditions [91,92]. Concerning turbidity (and TSS) increase significantly during and immediately after rainfall; algae increase results in higher water turbidity [53]. However, in the days before monitoring, there were no rainfall events, which explains the wetlands complex's low concentrations and turbidity values. The low TSS concentrations are associated with the dry season and low velocities in the wetlands that favor the retention time increase,

facilitating sedimentation and some pollutants removal, as well as a suspended solids decrease [3]. These TDS concentrations do not affect living organisms or water availability for human consumption [93–95]. Its measurement with other parameters allows fish yield estimation and biomass [96].

Variations in the NO_3 concentration may be due to runoff from the basin and wastewater from nearby municipalities [97]. It can also be associated with wastewater discharge, agriculture [98], and organic soils because they are a source of nitrates [99]. These types of soils are characteristic of lacustrine floodplains but don't cause eutrophication or human health risks [100]. An increase in NO_3 values was observed in the Guartinaja wetland, which might be due to low algal turbidity promoting nitrogen consumption [101], as well as the DO concentrations that help the nitrification process [3], since they promote the conversion of NH_4 to NO_3 [102]. Of all forms of N that can be present in water, NO_3 is the most available form of nitrogen for primary producers and is the best indicator when other forms of N are unavailable [6].

Phosphorus can accumulate in basins and be mobile even after restricting the sources that generate it [103]. Phosphorus inputs are also associated with aquifer geology since wetlands are fed directly or indirectly with groundwater that interacts with sulfur and iron biogeochemistry in the subsoil, causing phosphate eutrophication [104].

5. Conclusions

A multiple linear regression algorithm was implemented to generate empirical models considering water quality parameters and reflectance values from a Sentinel-2A satellite image. In this study, significant correlations were obtained between optically active parameters, TSS-Turbidity, which in turn correlated with optically inactive parameters, Turbidity-NO_3 and TSS-DO, as well as non-optically active parameters such as TDS-NO_3, TDS-TP.

Remote sensing combined with traditional water quality monitoring applied in the Guartinaja, Sapal and Momil wetlands proved efficient for estimating water quality parameters concentration without spectral response, such as NO_3 and TP. This possibility is due to transformation, interaction, and dependence processes existing between the different environmental variables in aquatic ecosystems. The decisive role played by turbidity in this water body type is highlighted, which acts as a connecting constituent that makes the water quality parameters estimation without spectral response by remote sensing feasible.

The empirical models obtained from the multiple regression analysis presented good fits, making the water quality parameters estimation without spectral response by remote sensing optimal because they have some bands between parameters pairs in common that show relationships such as TSS-DO with the B4, as well as Turbidity-NO_3 and TDS-NO_3 with the B6 and B8 bands.

The linear regressions' high fit values between measured and estimated data made it possible to obtain high spatial resolution concentration distribution maps to identify areas with high concentrations that could lead to intense alteration processes of the natural dynamics in the Bajo Sinú wetland complex.

Nitrogen and phosphorus (TP and NO_3) monitoring in wetlands is significant because they help to describe the wetland environmental status so that estimating them by combining remote sensing techniques and statistical tools generates inputs that properly represent the water body's real conditions; this reduces time and costs for monitoring, becoming an integral analysis alternative for the continuous supervision, preservation and possible adaptation forms of these aquatic ecosystems to climate change.

Author Contributions: C.P.-M. performed the literature review, processed the Sentinel-2 images to generate empirical models, analyzed results, and original draft preparation. F.T.-B. performed the experimental design and sampling campaigns, and directed the structure of the paper. G.C.-D. organized the methodology, analyzed the data statistically, and sampling campaigns. L.C.G.-M. revised the work critically for important intellectual content. All authors have read and agreed to the published version of the manuscript.

Funding: This research and The APC was funded by Research and Extension Department of University of Córdoba, Colombia. Grant number FI-01-19.

Data Availability Statement: The information and results of the project are not yet available. But, soon the project report will be available in the reposi-tory of the University of Cordoba.

Acknowledgments: The authors acknowledge and thanks the University of Córdoba, Colombia, for funding and supporting the research project FI-01-19 through its Research and Extension Department. This collaboration was invaluable for developing and obtaining these results.

Conflicts of Interest: The authors declare no conflict of interest.

References

1. Groot, D.; Brander, L.; Finlayson, M. Wetland Ecosystem Services. In *The Wetland Book*; Finlayson, C.M., Everard, M., Irvine, K., McInnes, R.J., Middleton, B.A., van Dam, A.A., Davidson, N.C., Eds.; Springer Netherlands: Dordrecht, The Netherlands, 2016; pp. 1–11. ISBN 978-94-007-6172-8.
2. Ritchie, W.; Neal, W.J.; Bush, D.; Pilkey, O.; Blasco, F.; Aizpuru, M.; Besnehard, J.; Bird, E.; Din, N.; Morton, R.A.; et al. *Encyclopedia of Coastal Science*; Encyclopedia of Earth Sciences Series; Springer International Publishing: New York, NY, USA, 2019; ISBN 978-3-319-93805-9.
3. Abiye, T. The Role of Wetlands Associated to Urban Micro-Dams in Pollution Attenuation, Johannesburg, South Africa. *Wetlands* **2015**, *35*, 1127–1136. [CrossRef]
4. Marotta, H.; Bento, L.; Esteves, F.D.A.; Enrich-Prast, A. Whole Ecosystem Evidence of Eutrophication Enhancement by Wetland Dredging in a Shallow Tropical Lake. *Estuaries Coasts* **2009**, *32*, 654–660. [CrossRef]
5. Palmer-Felgate, E.J.; Acreman, M.C.; Verhoeven, J.T.; Scholz, M.; Maltby, E.; Stratford, C.J.; Newman, J.; Miller, J.; Coughlin, D. How Effective Are Reedbeds, Ponds, Restored and Constructed Wetlands at Retaining Nitrogen, Phosphorus and Suspended Sediment from Agricultural Pollution in England? *Environ. Evid.* **2013**, *2*, 1. [CrossRef]
6. Sok, T.; Oeurng, C.; Kaing, V.; Sauvage, S.; Lu, X.; Pérez, J.M.S. Nutrient Transport and Exchange between the Mekong River and Tonle Sap Lake in Cambodia. *Ecol. Eng.* **2022**, *176*, 1645–1651. [CrossRef]
7. Rao, K.; Zhang, X.; Yi, X.-J.; Li, Z.-S.; Wang, P.; Huang, G.-W.; Guo, X.-X. Interactive Effects of Environmental Factors on Phytoplankton Communities and Benthic Nutrient Interactions in a Shallow Lake and Adjoining Rivers in China. *Sci. Total Environ.* **2018**, *619–620*, 1661–1672. [CrossRef]
8. Chang, N.-B.; Imen, S.; Vannah, B. Remote Sensing for Monitoring Surface Water Quality Status and Ecosystem State in Relation to the Nutrient Cycle: A 40-Year Perspective. *Crit. Rev. Environ. Sci. Technol.* **2015**, *45*, 101–166. [CrossRef]
9. Jia, Z.; Chang, X.; Duan, T.; Wang, X.; Wei, T.; Li, Y. Water Quality Responses to Rainfall and Surrounding Land Uses in Urban Lakes. *J. Environ. Manag.* **2021**, *298*, 113514. [CrossRef]
10. Nausch, M.; Woelk, J.; Kahle, P.; Nausch, G.; Leipe, T.; Lennartz, B. Phosphorus Fractions in Discharges from Artificially Drained Lowland Catchments (Warnow River, Baltic Sea). *Agric. Water Manag.* **2017**, *187*, 77–87. [CrossRef]
11. Nikolaidis, N.P.; Phillips, G.; Poikane, S.; Várbíró, G.; Bouraoui, F.; Malagó, A.; Lilli, M.A. River and Lake Nutrient Targets That Support Ecological Status: European Scale Gap Analysis and Strategies for the Implementation of the Water Framework Directive. *Sci. Total Environ.* **2022**, *813*, 151898. [CrossRef]
12. Zheng, Z.; Xu, Y.; Wang, J.; Li, Y.; Gu, B. Environmental Stress and Eutrophication in Freshwater Wetlands: Evidence from Carbon and Nitrogen Stable Isotopes in Cattail (Typha Domingensis Pers.). *Ecol. Process.* **2019**, *8*, 1–8. [CrossRef]
13. Breitburg, D.L.; Craig, J.K.; Fulford, R.S.; Rose, K.A.; Boynton, W.R.; Brady, D.C.; Ciotti, B.J.; Diaz, R.J.; Friedland, K.D.; Hagy, J.D.; et al. Nutrient Enrichment and Fisheries Exploitation: Interactive Effects on Estuarine Living Resources and Their Management. *Hydrobiologia* **2009**, *629*, 31–47. [CrossRef]
14. Poikane, S.; Portielje, R.; Denys, L.; Elferts, D.; Kelly, M.; Kolada, A.; Mäemets, H.; Phillips, G.; Søndergaard, M.; Willby, N.; et al. Macrophyte Assessment in European Lakes: Diverse Approaches but Convergent Views of 'Good' Ecological Status. *Ecol. Indic.* **2018**, *94*, 185–197. [CrossRef]
15. Wang, Q.; Rogers, M.J.; Ng, S.S.; He, J. Fixed Nitrogen Removal Mechanisms Associated with Sulfur Cycling in Tropical Wetlands. *Water Res.* **2021**, *189*, 116619. [CrossRef]
16. Hes, E.M.A.; van Dam, A.A. Modelling Nitrogen and Phosphorus Cycling and Retention in Cyperus Papyrus Dominated Natural Wetlands. *Environ. Model. Softw.* **2019**, *122*, 104531. [CrossRef]
17. Li, H.; Ma, X.; Zhou, B.; Ren, G.; Yuan, D.; Liu, H.; Wei, Z.; Gu, X.; Zhao, B.; Hu, Y.; et al. An Integrated Migration and Transformation Model to Evaluate the Occurrence Characteristics and Environmental Risks of Nitrogen and Phosphorus in Constructed Wetland. *Chemosphere* **2021**, *277*, 130219. [CrossRef] [PubMed]
18. Campo-Daza, G.A.; Zumaqué, L.; Torres-Bejarano, F.M. Efficiency Assessment of Constructed Wetlands for Fuel Contaminated Water Treatment. *Int. J. Environ. Sci. Technol.* **2021**, *19*, 12. [CrossRef]
19. González-Márquez, L.C.; Torres-Bejarano, F.M.; Rodríguez-Cuevas, C.; Torregroza-Espinosa, A.C.; Sandoval-Romero, J.A. Estimation of Water Quality Parameters Using Landsat 8 Images: Application to Playa Colorada Bay, Sinaloa, Mexico. *Appl. Geomat.* **2018**, *10*, 147–158. [CrossRef]

20. Elsayed, S.; Ibrahim, H.; Hussein, H.; Elsherbiny, O.; Elmetwalli, A.H.; Moghanm, F.S.; Ghoneim, A.M.; Danish, S.; Datta, R.; Gad, M. Assessment of Water Quality in Lake Qaroun Using Ground-Based Remote Sensing Data and Artificial Neural Networks. *Water* **2021**, *13*, 3094. [CrossRef]
21. Germán, A.; Shimoni, M.; Beltramone, G.; Rodríguez, M.I.; Muchiut, J.; Bonansea, M.; Scavuzzo, C.M.; Ferral, A. Space-Time Monitoring of Water Quality in an Eutrophic Reservoir Using SENTINEL-2 Data-A Case Study of San Roque, Argentina. *Remote Sens. Appl. Soc. Environ.* **2021**, *24*, 100614. [CrossRef]
22. Momen, B.; Eichler, L.W.; Boylen, C.W.; Zehr, J.P. Application of Multivariate Statistics in Detecting Temporal and Spatial Patterns of Water Chemistry in Lake George, New York. *Ecol. Model.* **1996**, *91*, 183–192. [CrossRef]
23. Mattikalli, N.M.; Richards, K.S. Estimation of Surface Water Quality Changes in Response to Land Use Change: Application of the Export Coefficient Model Using Remote Sensing and Geographical Information System. *J. Environ. Manag.* **1996**, *48*, 263–282. [CrossRef]
24. Wu, C.; Wu, J.; Qi, J.; Zhang, L.; Huang, H.; Lou, L.; Chen, Y. Empirical Estimation of Total Phosphorus Concentration in the Mainstream of the Qiantang River in China Using Landsat TM Data. *Int. J. Remote Sens.* **2010**, *31*, 2309–2324. [CrossRef]
25. Al-Shaibah, B.; Liu, X.; Zhang, J.; Tong, Z.; Zhang, M.; El-Zeiny, A.; Faichia, C.; Hussain, M.; Tayyab, M. Modeling Water Quality Parameters Using Landsat Multispectral Images: A Case Study of Erlong Lake, Northeast China. *Remote Sens.* **2021**, *13*, 1603. [CrossRef]
26. Deutsch, E.S.; Alameddine, I.; El-Fadel, M. Monitoring Water Quality in a Hypereutrophic Reservoir Using Landsat ETM+ and OLI Sensors: How Transferable Are the Water Quality Algorithms? *Environ. Monit. Assess.* **2018**, *190*, 141. [CrossRef] [PubMed]
27. González-Márquez, L.C.; Torres-Bejarano, F.M.; Torregroza-Espinosa, A.C.; Hansen-Rodríguez, I.R.; Rodríguez-Gallegos, H.B. Use of LANDSAT 8 Images for Depth and Water Quality Assessment of El Guájaro Reservoir, Colombia. *J. S. Am. Earth Sci.* **2018**, *82*, 231–238. [CrossRef]
28. Olmanson, L.G.; Bauer, M.E.; Brezonik, P.L. A 20-Year Landsat Water Clarity Census of Minnesota's 10,000 Lakes. *Remote Sens. Environ.* **2008**, *112*, 4086–4097. [CrossRef]
29. Robert, E.; Grippa, M.; Kergoat, L.; Pinet, S.; Gal, L.; Cochonneau, G.; Martinez, J.-M. Monitoring Water Turbidity and Surface Suspended Sediment Concentration of the Bagre Reservoir (Burkina Faso) Using MODIS and Field Reflectance Data. *Int. J. Appl. Earth Observ. Geoinf.* **2016**, *52*, 243–251. [CrossRef]
30. Torregroza-Espinosa, A.C.; Restrepo, J.C.; Correa-Metrio, A.; Hoyos, N.; Escobar, J.; Pierini, J.; Martínez, J.-M. Fluvial and Oceanographic Influences on Suspended Sediment Dispersal in the Magdalena River Estuary. *J. Mar. Syst.* **2020**, *204*, 103282. [CrossRef]
31. Maciel, D.A.; Barbosa, C.C.F.; de Moraes Novo, E.M.L.; Júnior, R.F.; Begliomini, F.N. Water Clarity in Brazilian Water Assessed Using Sentinel-2 and Machine Learning Methods. *ISPRS J. Photogramm. Remote Sens.* **2021**, *182*, 134–152. [CrossRef]
32. Sòria-Perpinyà, X.; Vicente, E.; Urrego, P.; Pereira-Sandoval, M.; Ruíz-Verdú, A.; Delegido, J.; Soria, J.M.; Moreno, J. Remote Sensing of Cyanobacterial Blooms in a Hypertrophic Lagoon (Albufera of València, Eastern Iberian Peninsula) Using Multitemporal Sentinel-2 Images. *Sci. Total Environ.* **2020**, *698*, 134305. [CrossRef]
33. Torres-Bejarano, F.M.; Arteaga-Hernández, F.; Rodríguez-Ibarra, D.; Mejía-Ávila, D.; González-Márquez, L.C. Water Quality Assessment in a Wetland Complex Using Sentinel 2 Satellite Images. *Int. J. Environ. Sci. Technol.* **2021**, *18*, 2345–2356. [CrossRef]
34. Casal, G. Assessment of Sentinel-2 to Monitor Highly Dynamic Small Water Bodies: The Case of Louro Lagoon (Galicia, NW Spain). *Oceanologia* **2022**, *64*, 88–102. [CrossRef]
35. Petus, C.; Waterhouse, J.; Lewis, S.; Vacher, M.; Tracey, D.; Devlin, M. A Flood of Information: Using Sentinel-3 Water Colour Products to Assure Continuity in the Monitoring of Water Quality Trends in the Great Barrier Reef (Australia). *J. Environ. Manag.* **2019**, *248*, 109255. [CrossRef] [PubMed]
36. Mortula, M.; Ali, T.; Bachir, A.; Elaksher, A.; Abouleish, M. Towards Monitoring of Nutrient Pollution in Coastal Lake Using Remote Sensing and Regression Analysis. *Water* **2020**, *12*, 1954. [CrossRef]
37. Torregroza-Espinosa, A.C.; Restrepo, J.C.; Escobar, J.; Brenner, M.; Newton, A. Nutrient Inputs and Net Ecosystem Productivity in the Mouth of the Magdalena River, Colombia. *Estuar. Coast. Shelf Sci.* **2020**, *243*, 106899. [CrossRef]
38. Bonansea, M.; Ledesma, M.; Bazán, R.; Ferral, A.; German, A.; O'Mill, P.; Rodriguez, C.; Pinotti, L. Evaluating the Feasibility of Using Sentinel-2 Imagery for Water Clarity Assessment in a Reservoir. *J. S. Am. Earth Sci.* **2019**, *95*, 102265. [CrossRef]
39. Isenstein, E.M.; Park, M.-H. Assessment of Nutrient Distributions in Lake Champlain Using Satellite Remote Sensing. *J. Environ. Sci.* **2014**, *26*, 1831–1836. [CrossRef]
40. Gao, Y.; Gao, J.; Yin, H.; Liu, C.; Xia, T.; Wang, J.; Huang, Q. Remote Sensing Estimation of the Total Phosphorus Concentration in a Large Lake Using Band Combinations and Regional Multivariate Statistical Modeling Techniques. *J. Environ. Manag.* **2015**, *151*, 33–43. [CrossRef]
41. Trinh, L.; Zablotskii, V.; Nguyen, T. Determining the Concentration of Suspended Sediment in the Lower Đáy River (Northern Vietnam) Using MSI Sentinel 2 High Spatial Resolution Data. *Izv. Atmos. Ocean. Phys.* **2020**, *56*, 1645–1651. [CrossRef]
42. Poikane, S.; Phillips, G.; Birk, S.; Free, G.; Kelly, M.G.; Willby, N.J. Deriving Nutrient Criteria to Support 'good' Ecological Status in European Lakes: An Empirically Based Approach to Linking Ecology and Management. *Sci. Total Environ.* **2019**, *650*, 2074–2084. [CrossRef]

43. Lasso, C.A.; Gutiérrez, F.D.P.; Morales, B.D. *Humedales Interiores de Colombia: Identificación, Caracterización y Establecimiento de Límites Según Criterios Biológicos y Ecológicos*; Instituto de Investigacion de Recursos Biológicos Alexander von Humboldt: Bogotá, Colombia, 2014; ISBN 978-958-8889-28-3.
44. Ministerio del Medio Ambiente. Política Nacional Para Humedales Interiores de Colombia 2002. Available online: https://faolex.fao.org/docs/pdf/col191716.pdf (accessed on 27 January 2013).
45. CVS Acuerdo de Consejo Directivo No. 76 2007. Available online: https://runap.parquesnacionales.gov.co/area-protegida/520 (accessed on 19 September 2022).
46. DANE. *Serie Municipal de Población Por Área, Para El Periodo 2018–2035*; Departamento Administrativo Nacional de Estadística: Bogotá, Columbia, 2020.
47. Barrientos Zuluaga, A.E.; Estrada Posada, A.J.; Vélez Flórez, G.L.; Vélez Upegui, J.I.; Racero Casarrubia, J.; Rios Góme, J.; Posada, J.A.; Caballero Acosta, J.H.; Giraldo, J.F.; Rios, L.; et al. *Plan de manejo y ordenamiento ambiental del complejo cenagoso del bajo Sinú*; Universidad Nacional, Sede Medellín: Medellín, Colombia, 2008; ISBN 978-958-8256-87-0.
48. Correa, P.; Vélez, J.; Smith, R.; Vélez, A.; Barrientos, A.; Gómez, J. Metodología de Balance Hídrico y de Sedimentos Como Herramienta de Apoyo Para La Gestión Integral Del Complejo Lagunar Del Bajo Sinú. *Av. Recur. Hidrául.* **2006**, *14*, 71–86.
49. Ávila, D.M.; Torres-Bejarano, F.M.; Lara, Z.M. Spectral Indices for Estimating Total Dissolved Solids in Freshwater Wetlands Using Semi-Empirical Models. A Case Study of Guartinaja and Momil Wetlands. *Int. J. Remote Sens.* **2022**, *43*, 2156–2184. [CrossRef]
50. Instituto De Hidrología, Meteorología Y Estudios Ambientales De Colombia. *IDEAM Guía Para El Monitoreo de Descargas, Aguas Superficiales y Subterráneas*; Instituto De Hidrología, Meteorología Y Estudios Ambientales De Colombia: Bogotá, Columbia, 2017.
51. Gascon, F.; Bouzinac, C.; Thépaut, O.; Jung, M.; Francesconi, B.; Louis, J.; Lonjou, V.; Lafrance, B.; Massera, S.; Gaudel-Vacaresse, A.; et al. Copernicus Sentinel-2A Calibration and Products Validation Status. *Remote Sens.* **2017**, *9*, 584. [CrossRef]
52. Olatunji, S.O. Modeling Optical Energy Gap of Strontium Titanate Multifunctional Semiconductor Using Stepwise Regression and Genetic Algorithm Based Support Vector Regression. *Comput. Mater. Sci.* **2021**, *200*, 110797. [CrossRef]
53. Rhyma, P.P.; Norizah, K.; Hamdan, O.; Faridah-Hanum, I.; Zulfa, A.W. Integration of Normalised Different Vegetation Index and Soil-Adjusted Vegetation Index for Mangrove Vegetation Delineation. *Remote Sens. Appl. Soc. Environ.* **2020**, *17*, 100280. [CrossRef]
54. Qu, X.; Chen, Y.; Liu, H.; Xia, W.; Lu, Y.; Gang, D.D.; Lin, L.S. A Holistic Assessment of Water Quality Condition and Spatiotemporal Patterns in Impounded Lakes along the Eastern Route of China's South-to-North Water Diversion Project. *Water Res.* **2020**, *185*, 116275. [CrossRef] [PubMed]
55. Wu, J.-L.; Ho, C.-R.; Huang, C.-C.; Srivastav, A.; Tzeng, J.-H.; Lin, Y.-T. Hyperspectral Sensing for Turbid Water Quality Monitoring in Freshwater Rivers: Empirical Relationship between Reflectance and Turbidity and Total Solids. *Sensors* **2014**, *14*, 22670–22688. [CrossRef]
56. Brezonik, P.; Menken, K.D.; Bauer, M. Landsat-Based Remote Sensing of Lake Water Quality Characteristics, Including Chlorophyll and Colored Dissolved Organic Matter (CDOM). *Lake Reserv. Manag.* **2005**, *21*, 373–382. [CrossRef]
57. Butler, B.A.; Ford, R.G. Evaluating Relationships between Total Dissolved Solids (TDS) and Total Suspended Solids (TSS) in a Mining-Influenced Watershed. *Mine Water Environ.* **2018**, *37*, 18–30. [CrossRef]
58. Adusei, Y.Y.; Quaye-Ballard, J.; Adjaottor, A.A.; Mensah, A.A. Spatial Prediction and Mapping of Water Quality of Owabi Reservoir from Satellite Imageries and Machine Learning Models. *Egypt. J. Remote Sens. Sp. Sci.* **2021**, *24*, 825–833. [CrossRef]
59. Geng, M.; Wang, K.; Yang, N.; Li, F.; Zou, Y.; Chen, X.; Deng, Z.; Xie, Y. Spatiotemporal Water Quality Variations and Their Relationship with Hydrological Conditions in Dongting Lake after the Operation of the Three Gorges Dam, China. *J. Clean. Prod.* **2021**, *283*, 124644. [CrossRef]
60. Ji, G.; Havens, K. Periods of Extreme Shallow Depth Hinder but Do Not Stop Long-Term Improvements of Water Quality in Lake Apopka, Florida (USA). *Water* **2019**, *11*, 538. [CrossRef]
61. Pérez-Vásquez, N.D.S.; Arias-Rios, J.; Quirós-Rodríguez, J.A. Variación Espacio-Temporal de Plantas Vasculares Acuáticas en el Complejo Cenagoso del Bajo Sinú, Córdoba, Colombia. *Acta Biol. Colomb.* **2015**, *20*, 155–165. [CrossRef]
62. Hou, X.; Feng, L.; Duan, H.; Chen, X.; Sun, D.; Shi, K. Fifteen-Year Monitoring of the Turbidity Dynamics in Large Lakes and Reservoirs in the Middle and Lower Basin of the Yangtze River, China. *Remote Sens. Environ.* **2017**, *190*, 107–121. [CrossRef]
63. Balasubramanian, S.V.; Pahlevan, N.; Smith, B.; Binding, C.; Schalles, J.; Loisel, H.; Gurlin, D.; Greb, S.; Alikas, K.; Randla, M.; et al. Robust Algorithm for Estimating Total Suspended Solids (TSS) in Inland and Nearshore Coastal Waters. *Remote Sens. Environ.* **2020**, *246*, 111768. [CrossRef]
64. Salcedo-Hernández, M.J.; Duque, S.R.; Palma, L.; Torres-Bejarano, A.; Montenegro, D.; Bahamón, N.; Lagos, L.; Alvarado, L.F.; Gómez, M.; Alba, A.P. Ecología del fitoplancton y dinámica hidrológica del sistema lagunar de Yahuarcaca, Amazonas, Colombia: Análisis integrado de 16 años de estudio. *Mundo Amazón.* **2012**, *3*, 9–41.
65. Torres-Bejarano, A.M.; Duque, S.R.; Caraballo-Gracia, P.R. Heterogeneidad Espacial y Temporal de las Condiciones Físicas y Químicas de dos Lagos de Inundación en la Amazonia Colombiana. *Actual. Biol.* **2013**, *35*, 63–76. [CrossRef]
66. Torres-Bejarano, F.M.; Torregroza-Espinosa, A.C.; Martinez-Mera, E.; Castañeda-Valbuena, D.; Tejera-Gonzalez, M.P. Hydrodynamics and Water Quality Assessment of a Coastal Lagoon Using Environmental Fluid Dynamics Code Explorer Modeling System. *Glob. J. Environ. Sci. Manag.* **2020**, *6*, 289–308. [CrossRef]
67. Duque, G.; Gamboa-García, D.E.; Molina, A.; Cogua, P. Effect of Water Quality Variation on Fish Assemblages in an Anthropogenically Impacted Tropical Estuary, Colombian Pacific. *Environ. Sci. Pollut. Res.* **2020**, *27*, 25740–25753. [CrossRef]

68. Aguirre, S.E.; Piraneque, N.V.; Linero-Cueto, J. Concentración de metales pesados y calidad fisicoquímica del agua de la Ciénaga Grande de Santa Marta. *Rev. U.D.C.A Actual. Divulg. Cient.* **2021**, *24*, 1–10. [CrossRef]
69. Muñoz-López, C.L.; Rivera-Rondón, C.A. Diatom Response to Environmental Gradients in the High Mountain Lakes of the Colombia's Eastern Range. *Aquat. Sci.* **2021**, *84*, 15. [CrossRef]
70. Torres-Bejarano, F.; García-Gallego, J.; Salcedo-Salgado, J. Numerical Modeling of Nutrient Transport to Assess the Agricultural Impact on the Trophic State of Reservoirs. *Int. Soil Water Conserv. Res.* **2023**, *11*, 197–212. [CrossRef]
71. Das, R.; Krishnakumar, A.; Kumar, M.R.; Thulseedharan, D. Water Quality Assessment of Three Tropical Freshwater Lakes of Kerala, SW India, with Special Reference to Drinking Water Potential. *Environ. Nanotechnol. Monit. Manag.* **2021**, *16*, 100588. [CrossRef]
72. Gopal, V.; Achyuthan, H.; Jayaprakash, M. Hydrogeochemical Characterization of Yercaud Lake Southern India: Implications on Lake Water Chemistry through Multivariate Statistics. *Acta Ecol. Sin.* **2018**, *38*, 200–209. [CrossRef]
73. Li, S.-L.; Xu, S.; Wang, T.-J.; Yue, F.-J.; Peng, T.; Zhong, J.; Wang, L.-C.; Chen, J.-A.; Wang, S.-J.; Chen, X.; et al. Effects of Agricultural Activities Coupled with Karst Structures on Riverine Biogeochemical Cycles and Environmental Quality in the Karst Region. *Agric. Ecosyst. Environ.* **2020**, *303*, 107120. [CrossRef]
74. Zhao, Y.; Xia, X.H.; Yang, Z.F.; Wang, F. Assessment of Water Quality in Baiyangdian Lake Using Multivariate Statistical Techniques. *Procedia Environ. Sci.* **2012**, *13*, 1213–1226. [CrossRef]
75. Shi, Z.; Xu, J.; Huang, X.; Zhang, X.; Jiang, Z.; Ye, F.; Liang, X. Relationship between Nutrients and Plankton Biomass in the Turbidity Maximum Zone of the Pearl River Estuary. *J. Environ. Sci.* **2017**, *57*, 72–84. [CrossRef]
76. Smith, V.H.; Shapiro, J. Chlorophyll-Phosphorus Relations in Individual Lakes. Their Importance to Lake Restoration Strategies. *Environ. Sci. Technol.* **1981**, *15*, 444–451. [CrossRef]
77. Quinlan, R.; Filazzola, A.; Mahdiyan, O.; Shuvo, A.; Blagrave, K.; Ewins, C.; Moslenko, L.; Gray, D.K.; O'Reilly, C.M.; Sharma, S. Relationships of Total Phosphorus and Chlorophyll in Lakes Worldwide. *Limnol. Oceanogr.* **2021**, *66*, 392–404. [CrossRef]
78. Pu, J.; Wang, S.; Ni, Z.; Wu, Y.; Liu, X.; Wu, T.; Wu, H. Implications of Phosphorus Partitioning at the Suspended Particle-Water Interface for Lake Eutrophication in China's Largest Freshwater Lake, Poyang Lake. *Chemosphere* **2021**, *263*, 128334. [CrossRef]
79. Chawla, I.; Karthikeyan, L.; Mishra, A.K. A Review of Remote Sensing Applications for Water Security: Quantity, Quality, and Extremes. *J. Hydrol.* **2020**, *585*, 124826. [CrossRef]
80. Kulshreshtha, A.; Shanmugam, P. Assessment of Trophic State and Water Quality of Coastal-Inland Lakes Based on Fuzzy Inference System. *J. Great Lakes Res.* **2018**, *44*, 1010–1025. [CrossRef]
81. Li, W.; Dou, Z.; Cui, L.; Wang, R.; Zhao, Z.; Cui, S.; Lei, Y.; Li, J.; Zhao, X.; Zhai, X. Suitability of Hyperspectral Data for Monitoring Nitrogen and Phosphorus Content in Constructed Wetlands. *Remote Sens. Lett.* **2020**, *11*, 495–504. [CrossRef]
82. Salama, M.S.; Radwan, M.; van der Velde, R. A Hydro-Optical Model for Deriving Water Quality Variables from Satellite Images (HydroSat): A Case Study of the Nile River Demonstrating the Future Sentinel-2 Capabilities. *Phys. Chem. Earth Parts A/B/C* **2012**, *50–52*, 224–232. [CrossRef]
83. Sharaf, E.; Zhang, Y.; Suliman, A. Mapping Concentrations of Surface Water Quality Parameters Using a Novel Remote Sensing and Artificial Intelligence Framework. *Int. J. Remote Sens.* **2017**, *38*, 1023–1042. [CrossRef]
84. Chi, L.; Song, X.; Yuan, Y.; Wang, W.; Cao, X.; Wu, Z.; Yu, Z. Main Factors Dominating the Development, Formation and Dissipation of Hypoxia off the Changjiang Estuary (CE) and Its Adjacent Waters, China. *Environ. Pollut.* **2020**, *265*, 115066. [CrossRef] [PubMed]
85. Vakili, T.; Amanollahi, J. Determination of Optically Inactive Water Quality Variables Using Landsat 8 Data: A Case Study in Geshlagh Reservoir Affected by Agricultural Land Use. *J. Clean. Prod.* **2020**, *247*, 119134. [CrossRef]
86. Li, Y.; Zhang, Y.; Shi, K.; Zhu, G.; Zhou, Y.; Zhang, Y.; Guo, Y. Monitoring Spatiotemporal Variations in Nutrients in a Large Drinking Water Reservoir and Their Relationships with Hydrological and Meteorological Conditions Based on Landsat 8 Imagery. *Sci. Total Environ.* **2017**, *599–600*, 1705–1717. [CrossRef] [PubMed]
87. Lehmann, M.K.; Schütt, E.M.; Hieronymi, M.; Dare, J.; Krasemann, H. Analysis of Recurring Patchiness in Satellite-Derived Chlorophyll a to Aid the Selection of Representative Sites for Lake Water Quality Monitoring. *Int. J. Appl. Earth Observ. Geoinf.* **2021**, *104*, 102547. [CrossRef]
88. Li, S.; Song, K.; Wang, S.; Liu, G.; Wen, Z.; Shang, Y.; Lyu, L.; Chen, F.; Xu, S.; Tao, H.; et al. Quantification of Chlorophyll-a in Typical Lakes across China Using Sentinel-2 MSI Imagery with Machine Learning Algorithm. *Sci. Total Environ.* **2021**, *778*, 146271. [CrossRef]
89. Kim, T.; Sheng, Y.P.; Park, K. Modeling Water Quality and Hypoxia Dynamics in Upper Charlotte Harbor, Florida, U.S.A. during 2000. *Estuar. Coast. Shelf Sci.* **2010**, *90*, 250–263. [CrossRef]
90. Kim, Y.H.; Son, S.; Kim, H.C.; Kim, B.; Park, Y.G.; Nam, J.; Ryu, J. Application of Satellite Remote Sensing in Monitoring Dissolved Oxygen Variabilities: A Case Study for Coastal Waters in Korea. *Environ. Int.* **2020**, *134*, 105301. [CrossRef] [PubMed]
91. Randall, G.W.; Goss, M.J. Nitrate Losses to Surface Water Through Subsurface, Tile Drainage. *Nitrogen Environ.* **2008**, 145–175. [CrossRef]
92. Camargo, J.A.; Alonso, Á. Ecological and Toxicological Effects of Inorganic Nitrogen Pollution in Aquatic Ecosystems: A Global Assessment. *Environ. Int.* **2006**, *32*, 831–849. [CrossRef]
93. Weber-Scannell, P.; Duffy, L. Effects of Total Dissolved Solids on Aquatic Organisms: A Review of Literature and Recommendation for Salmonid Species. *Am. J. Environ. Sci.* **2007**, *3*, 1–6. [CrossRef]

94. Weber-Scannell, P.K.; Jacobs, L. *Effects of Total Dissolved on Aquiatic Organisms*; Technical Report No. 01–06; Alaska Department of Fish and Game Division of Habitat and Restoration: Anchorage, AK, USA, 2001.
95. WHO. *Guidelines for Drinking Water Quality*, 4th ed.; World Health Organization: Geneva, Switzerland, 2017.
96. Hanson, J.M.; Leggett, W.C. Empirical Prediction of Fish Biomass and Yield. *Can. J. Fish. Aquat. Sci.* **1982**, *39*, 257–263. [CrossRef]
97. Lim, J.; Choi, M. Assessment of Water Quality Based on Landsat 8 Operational Land Imager Associated with Human Activities in Korea. *Environ. Monit. Assess.* **2015**, *187*, 384. [CrossRef]
98. Amarnath, G.; Matheswaran, K.; Pandey, P.; Alahacoon, N.; Yoshimoto, S. Flood Mapping Tools for Disaster Preparedness and Emergency Response Using Satellite Data and Hydrodynamic Models: A Case Study of Bagmathi Basin, India. *Proc. Natl. Acad. Sci. India Sect. A Phys. Sci.* **2017**, *87*, 941–950. [CrossRef]
99. Hu, M.; Wang, Y.; Du, P.; Shui, Y.; Cai, A.; Lv, C.; Bao, Y.; Li, Y.; Li, S.; Zhang, P. Tracing the Sources of Nitrate in the Rivers and Lakes of the Southern Areas of the Tibetan Plateau Using Dual Nitrate Isotopes. *Sci. Total Environ.* **2019**, *658*, 132–140. [CrossRef]
100. Nevada Division of Environmental Protection. *NDEP Nevada's Nutrient Criteria Strategy–Version 2*; Nevada Division of Environmental Protection Bureau of Water Quality Planning: Carson, Nevada, 2009.
101. Zou, W.; Zhu, G.; Cai, Y.; Vilmi, A.; Xu, H.; Zhu, M.; Gong, Z.; Zhang, Y.; Qin, B. Relationships between Nutrient, Chlorophyll a and Secchi Depth in Lakes of the Chinese Eastern Plains Ecoregion: Implications for Eutrophication Management. *J. Environ. Manag.* **2020**, *260*, 109923. [CrossRef]
102. Rak, A.E.; Kari, Z.A.; Ramli, M.Z.; Harun, H.C.; Sukri, S.A.M.; Khalid, H.N.M.; Abdullah, F.; Dawood, M.A.O.; Wee, W.; Wei, L.S. The Impact of Water Quality on the Asian Clam, Corbicula Fluminea, Distribution in Pergau Lake, Kelantan, Malaysia. *Saudi J. Biol. Sci.* **2022**, *29*, 2348–2354. [CrossRef] [PubMed]
103. Powers, S.M.; Bruulsema, T.W.; Burt, T.P.; Chan, N.I.; Elser, J.J.; Haygarth, P.M.; Howden, N.J.K.; Jarvie, H.P.; Lyu, Y.; Peterson, H.M.; et al. Long-Term Accumulation and Transport of Anthropogenic Phosphorus in Three River Basins. *Nat. Geosci.* **2016**, *9*, 353–356. [CrossRef]
104. Smolders, A.J.P.; Lucassen, E.C.H.E.T.; Bobbink, R.; Roelofs, J.G.M.; Lamers, L.P.M. How Nitrate Leaching from Agricultural Lands Provokes Phosphate Eutrophication in Groundwater Fed Wetlands: The Sulphur Bridge. *Biogeochemistry* **2010**, *98*, 1–7. [CrossRef]